Iranian Polymer Journal
15 (3), 2006, 183-193

Available online at: http://journal.ippi.ac.ir

Viscoelastic Buckling of Euler-Bernoulli and Timoshenko Beams under Time Variant General Loading Conditions

Manouchehr Salehi* and Faroukh Ansari

Mechanical Engineering Department, Amir Kabir University of Technology
P.O. Box: 15875-4413, Tehran, I.R. Iran

Received 6 February 2005; accepted 31 January 2006

ABSTRACT

A comprehensive study on the linear viscoelastic buckling of Euler-Bernoulli (E-B) and Timoshenko beams is presented. The mathematical formulation for visco elastic E-B beam under combined time variant general axial and transverse loading and for the viscoelastic Timoshenko beam only subjected to time variant general axial loading is developed. Various boundary conditions are defined then clamped edge constraints are applied. The E-B and Timoshenko cantilever beams are investigated under general axial loading. Both differential and integral forms of the beam governing equations are derived, but only the differential equations are solved, using the finite difference numerical technique assuming Kelvin material model. A computer programme is implemented for computing the beam deflections and a technique is described for obtaining the critical buckling loads. Where possible the finite difference numerical results are compared with other available results. The correlations of the results are extremely well. The important contributing factors are the general nature of the loading and the technique for calculating the critical buckling loads.

Key Words:
Euler-Bernoulli beam;
Timoshenko beam;
viscoelastic beam;
critical buckling load;
finite-difference;
Kelvin model.

(*) To whom correspondence to be addressed.
E-mail: msalehi@aut.ac.ir

INTRODUCTION

Many different types of analyses for elastic and plastic behaviour for isotropic [1], and anisotropic E-B and Timoshenko beams have been carried out [2]. An analytical model to predict the linear viscoelastic behaviour of thin-walled laminated fibre-reinforced plastic (FRP) composite beams is presented [2]. Correspondence principle is used and the model integrates micro/macro-mechanics of composites and mechanics of thin-walled laminated beams to perform beam analysis in

Laplace or Carson domain. Results for a box-beam in tension and under bending are obtained. A Maxwell solid and three parameter solid type models are used to study the bending behaviour of viscous material in higher-order elastic beams by Johnson and Tessler [3]. A viscoelstic internal variable constitutive theory is applied to both the beam theory and the finite element formulation. Finally, numerical examples for the problems of relaxation, creep and cyclic creep are presented for an orthotropic Maxwell type solid beam [3]. However, viscoelastic behaviour of beams, in particular Timoshenko beams, has received a minor attention in compression. Recently, the creep buckling of linear viscoelastic E-B beam under axial and transverse loads is carried out [4]. A Maxwell model material is used for investigating the behaviour of nuclear fuel rods at elevated temperatures. The quasi-static and dynamic analysis of viscoelastic Timoshenko beam using the hybrid Laplace transform/finite element method is presented by Chen [5]. The limited study observed in this field encouraged the first author to undertake a comprehensive study on the linear viscoelastic buckling behaviour of E-B and Timoshenko beams subjected to time variant general loading conditions. In very special cases, analytical solutions are presented for solving Maxwell type fluid material model [4].

With increasing the application of polymer based materials in several fields of engineering like mechanical, aerospace, electrical poles etc. [6,7], and the increasingly common use of such material in structural elements like beams, columns, plates and shells, it seems reasonable to start investigating the mechanical behaviour of these types of elements. Polymer based resins are used in composite structures, in which viscoelastic behaviour ought to be considered. For metal structures at elevated temperatures viscoelastic type of analysis is essential.

In the following sections of the paper, beam governing equations, loading functions, boundary conditions and the mechanical properties of the Kelvin model viscoelastic material are given. The finite difference formulation and the numerical solutions of the beam governing equations together with comparison results and seven examples are presented in the following sections.

BEAM COORDINATE SYSTEM AND LOADING

The coordinate system and the loading are shown in Figure 1 for combined axial and transverse loading and in Figure 2 for axial loading only. The deformed shape of the beam is highly exaggerated. In Figure 1 the beam can be loaded with point loads at different locations along the length of the beam as axial and transverse loads as well as non-uniformly distributed loads in both axial and transverse directions. This type of loading is used for E-B beam.

For Timoshenko beam a similar type of loading as above is used but only in axial direction, as is shown in Figure 2.

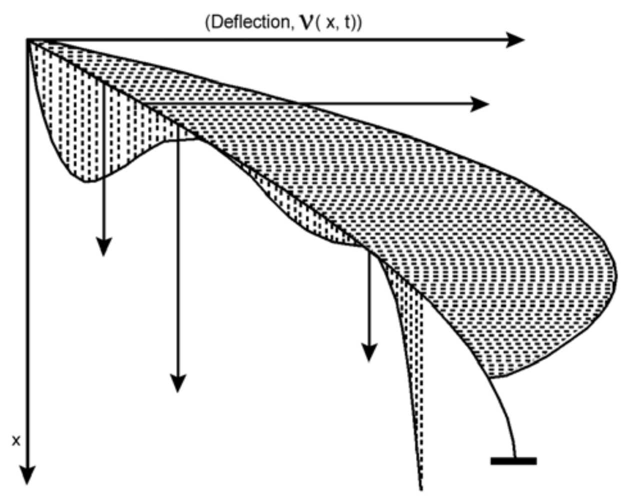

Figure 1. Loading on Euler-Bernoulli beam.

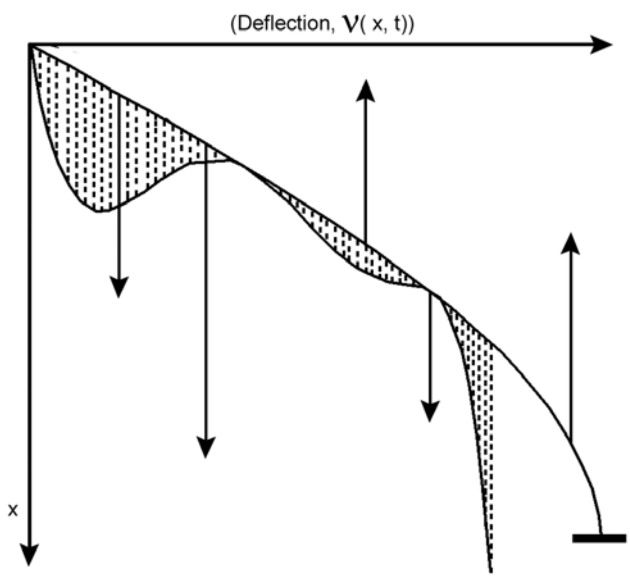

Figure 2. Loading on Timoshenko beam.

BEAM DIFFERENTIAL EQUATIONS

The deflection variation of every point of the beam is due to bending only in E-B beam and due to combined bending and shear in Timoshenko beam.

Euler-Bernoulli Beam Differential Equations

The bending moment due to axial load and transverse load is given as follows:

$$M = M^F + M^q \quad (1)$$

where M^F and M^q are bending moments due to axial and distributed transverse loads, respectively. The bending moments are in terms of time and position along the beam length. The bending moment equations due to general axial and transverse loadings are given as:

$$M^F = \int_o^x [\upsilon(x,t) - \upsilon(x',t)] \cdot F(x',t) \cdot dx' \quad (2)$$

$$M^q = \int_o^x (x - x') \cdot q(x',t) \cdot dx' \quad (3)$$

where $\upsilon(x,t)$ is the deflection function, $F(x,t)$ is the axial load profile and $q(x,t)$ is the transverse load profile. The loading function includes point, distributed and couple type of loading. Consequently, eqn (1) can be written as:

$$M_{(x,t)} = \int_o^x [\upsilon(x,t) - \upsilon(x',t)] \cdot F(x',t) \cdot dx' + \int_o^x (x - x') \cdot q(x',t) \cdot dx' \quad (4)$$

The relation between the beam deflection and bending moment [8] given below:

$$P^E(M_{(x,t)}) = Q^E (I.\upsilon''_{(x,t)}) \quad (5)$$

where the differential operators are stated as follows:

$$P^E = \sum_{i=0}^{n} p_i^E \cdot \frac{\partial^i}{\partial t^i} \ , \ Q^E = \sum_{i=0}^{n} q_i^E \cdot \frac{\partial^i}{\partial t^i}$$

Now substituting eqn (4) into eqn (5) results the following general equation:

$$P^E\left(\int_o^x [\upsilon(x,t) - \upsilon(x',t)] \cdot F(x',t) \cdot dx' + \int_o^x (x - x') \cdot q(x',t) \cdot dx' \right) = Q^E\left(I_{(x,t)} \cdot \frac{\partial^2 \upsilon_{(x,t)}}{\partial x^2} \right) \quad (6)$$

where I is the second moment of area of the beam cross-section. This is the most general equation for Euler-Bernoulli beam at uniform temperature.

In the especial case of constant cross-section with respect to time and neglecting the Poisson effect [8], eqn (6) becomes:

$$P^E\left(\int_o^x [\upsilon(x,t) - \upsilon(x',t)] \cdot F(x',t) \cdot dx' + \int_o^x (x - x') \cdot q(x',t) \cdot dx' \right) = I_{(x)} \cdot Q^E\left(\frac{\partial^2 \upsilon_{(x,t)}}{\partial x^2} \right) \quad (7)$$

In the case of pure transverse loading, eqn (7) changes to:

$$P^E\left(\int_o^x (x - x') \cdot q(x',t) \cdot dx' \right) = I_{(x)} \cdot Q^E\left(\frac{\partial^2 \upsilon_{(x,t)}}{\partial x^2} \right) \quad (8)$$

and in the case of pure axial loading, eqn (7) becomes:

$$P^E\left(\int_o^x [\upsilon(x,t) - \upsilon(x',t)] \cdot F(x',t) \cdot dx' \right) = I_{(x)} \cdot Q^E\left(\frac{\partial^2 \upsilon_{(x,t)}}{\partial x^2} \right) \quad (9)$$

Timoshenko Beam Differential Equations

The deflection of every point of the beam is due to bending and shear. In homogeneous and isotropic linear viscoelastic material at uniform temperature the deformations due to bending and shear are independent [8]. Consequently the process of deformation can be shown to be as follows:

$$\frac{\partial^i \partial^j \upsilon_{(x,t)}}{\partial t^i \partial x^j} = \left. \frac{\partial^i \partial^j \upsilon_{(x,t)}}{\partial t^i \partial x^j} \right|_M + \left. \frac{\partial^i \partial^j \upsilon_{(x,t)}}{\partial t^i \partial x^j} \right|_S \quad (10)$$

The indices M and S refer respectively to bending and shear effects. Each term in eqn (10) can be separately evaluated.

a: Bending Effect

The relationship between the bending moment and the axial load can be shown to be as follows:

$$P^E\left(\int_o^x [\upsilon(x,t)-\upsilon(x',t)]F(x',t)dx'\right)= Q^E\left(I_{(x,t)}\cdot\frac{\partial^2\upsilon^M_{(x,t)}}{\partial x^2}\right) \quad (11)$$

To make eqn (11) suitable for the application of boundary conditions it is differentiated twice with respect to as follows:

$$\frac{\partial^2}{\partial x^2}P^E\left(\int_o^x [\upsilon(x,t)-\upsilon(x',t)]F(x',t)dx'\right)= Q^E\left(I_{(x,t)}\cdot\frac{\partial^4\upsilon^M_{(x,t)}}{\partial x^4}\right) \quad (12)$$

b: Shear Effect

The rate of change of the slope (or curvature) due to shear for the linear elastic beam in terms of internal axial force is [9]:

$$\frac{\partial^2\upsilon^S}{\partial x^2}=\frac{nN}{AG}\cdot\frac{\partial^2\upsilon}{\partial x^2} \quad (13)$$

where n is the shear correction factor, υ^s is the deflection due to shear, N is the internal axial force, A is the cross sectional area and G is the shear modulus of elasticity. A similar equation can be obtained for a linear viscoelastic material. This equation in Laplace space is found to be as follows:

$$\overline{\upsilon''}^S=\frac{n\overline{N}}{A\left(\dfrac{\overline{Q}^G(s)}{\overline{P}^G(s)}\right)}\cdot\overline{\upsilon''} \quad (14)$$

where $\overline{Q}^G$ and $\overline{P}^G$ are differential operators due to shear strain and shear stress, respectively and:

$$\upsilon''=\frac{\partial^2\upsilon}{\partial x^2},\ \upsilon''^S=\frac{\partial^2\upsilon^S}{\partial x^2}$$

Eqn (14) can be written as:

$$\overline{P}^G(s)\cdot\frac{n\overline{N}}{A}\cdot\overline{\upsilon''}=\overline{Q}^G(s)\cdot\overline{\upsilon''}^S \quad (15)$$

or in inverse Laplace transform as:

$$P^G\left(\frac{nN}{A}\cdot\upsilon''\right)=Q^G(\upsilon''^S) \quad (16)$$

Finally, the equation relating the deflection due to shear and the axial force is found to be as follows:

$$P^G\left(\frac{n}{A}\cdot\left(\int_o^x F_{(x',t)}\cdot dx'\right)\cdot\frac{\partial^4\upsilon}{\partial x^4}\right)=Q^G\left(\frac{\partial^4\upsilon^S}{\partial x^4}\right) \quad (17)$$

Consequently, eqns (10), (12) and (17) constitute the beam differential equations.

Mechanical Properties for Kelvin Model Material

In Kelvin model the operators P^E and Q^E which are restated as follows:

$$P^E=\sum_{i=0}^{n}p_i^E.\partial^i/\partial t^i\ ,\ Q^E=\sum_{i=0}^{n}q_i^E.\partial^i/\partial t^i$$

are assumed to have values as given below:

$$P_o^{EK}=1,\ P_i^{EK}=0,\quad (i>0)$$
$$q_o^{EK}=E,\ q_1^{EK}=\eta,\ q_1^{EK}=0,\quad (i>0) \quad (18)$$

the superscripts K refer to Kelvin. Neglecting the effect of Poisson ratio, we obtain:

$$P^{vk}=1,\ Q^{vk}=0 \quad (19)$$

The ratio of the operators due to shear are then as follows:

$$\frac{Q^{GK}}{P^{GK}}=\frac{\dfrac{Q^{EK}}{P^{EK}}}{1+\dfrac{Q^{vK}}{P^{vK}}} \quad (20)$$

thus we conclude that:

$$P^{GK}=1$$
$$Q^{GK}=E+\eta\frac{\partial}{\partial t} \quad (21)$$

where E is the modulus of elasticity and η is the viscosity coefficient.

Now substituting the properties obtained in eqns (18), (19) and (21) in eqns (12) and (17) the differential forms of the equations become:

$$\int_{o}^{x}\left[\upsilon(x,t)-\upsilon(x',t)\right]\cdot F(x',t)\cdot dx' = I_{(x)}(E+\eta\frac{\partial}{\partial t})(\upsilon''^{M}_{(x,t)}) \quad (22)$$

$$\left(\int_{o}^{x}F_{(x',t)}\cdot dx'\right)\cdot\upsilon''_{(x,t)}=\frac{A_{(x)}}{n}(E+\eta\frac{\partial}{\partial t})(\upsilon''^{S}_{(x,t)}) \quad (23)$$

the integral form of the equations transform to:

$$\upsilon''^{M}_{(x,t)}=\frac{1}{I_{(x)}}\int_{o}^{t}J^{EK}(t-t')\cdot\frac{\partial M^{F}_{(x,t')}}{\partial t'}\cdot dt' \quad (24)$$

$$\upsilon''^{S}=\frac{n}{A}\int_{o}^{t}J^{GK}(t-t')\cdot\frac{\partial\left(\left(\int_{o}^{x}F_{(x',t')}\cdot dx'\right)\cdot\upsilon''\right)}{\partial t'}\cdot dt' \quad (25)$$

Boundary Conditions

Using the following equations, the boundary conditions are defined:

$$P^{E}\left(\frac{\partial^2 M^{F}}{\partial x^2}\right)=I_{(x)}Q^{E}\left(\frac{\partial^4\upsilon^{M}_{(x,t)}}{\partial x^4}\right) \quad (26)$$

$$\frac{n}{A}P^{G}\left(\frac{\partial^2}{\partial x^2}\left(\int_{o}^{x}F_{(x',t)}\cdot dx'\right)\cdot\frac{\partial^4\upsilon}{\partial x^4}\right)=Q^{G}\left(\frac{\partial^4\upsilon^{S}}{\partial x^4}\right) \quad (27)$$

(a) Clamped

$\upsilon = 0$

$$\frac{\partial\upsilon}{\partial x}=0 \quad (28)$$

The total deflection curve has a zero slope at the clamped edge. The deflection can include shear effect or it may be solely due to bending.

(b) Internal Support

$\upsilon = 0$

$$\left.\frac{\partial\upsilon}{\partial x}\right|_{x_o^-}=\left.\frac{\partial\upsilon}{\partial x}\right|_{x_o^+} \quad (29)$$

A similar explanation as that given above for the deflection is valid here too. The second of eqn (29) shows that at the support the slope is continuous.

NUMERICAL SOLUTION

Beam Governing Differential Equations

The closed form solution of the E-B beam governing equations for Maxwell model is presented by Yu [4]. However, this solution is only obtained for a special loading and boundary conditions. Here, on the other hand, a very general loading for E-B and Timoshenko beams with variable time is assumed for a Kelvin material model.

The governing differential equations for E-B and Timoshenko beams, i.e. eqns (7), (10), (12) and (17) are solved utilizing the finite difference numerical solution technique for obtaining the numerical results. In order to minimize the computational effort, the E-B beam governing equation is not discretized instead the Timoshenko beam governing equations are written in finite difference form, where E-B beam results are required the shear term in the Timoshenko beam equations is ignored. Consequently, only eqns (10), (12) and (17) are stated in finite difference form (Figure 3) as follows:

$$\Delta\upsilon''_{(x,t)}=\Delta\upsilon''^{M}_{(x,t)}+\Delta\upsilon''^{S}_{(x,t)} \quad (30)$$

$$\Delta\upsilon''^{M}_{(x,t)}=\frac{\left[\sum_{i=o}^{i=\frac{x}{\Delta x}}(\upsilon''_{(x,t-\Delta t)}-\upsilon''_{(i\cdot\Delta x,t-\Delta t)})\cdot F_{(i\cdot\Delta x,t)}\cdot\Delta x\right]-IE\upsilon''^{M}_{(x,t-\Delta t)}}{I\eta}\cdot\Delta t \quad (31)$$

$$\Delta\upsilon''^{S}_{(x,t)}=\frac{\left[\sum_{i=o}^{i=\frac{x}{\Delta x}}F_{(i\Delta x,t)}\cdot\Delta x\right]\cdot\upsilon''_{(x,t)}-\frac{AE}{n}\cdot\upsilon''^{S}_{(x,t-\Delta t)}}{\frac{A\eta}{n}}\cdot\Delta t \quad (32)$$

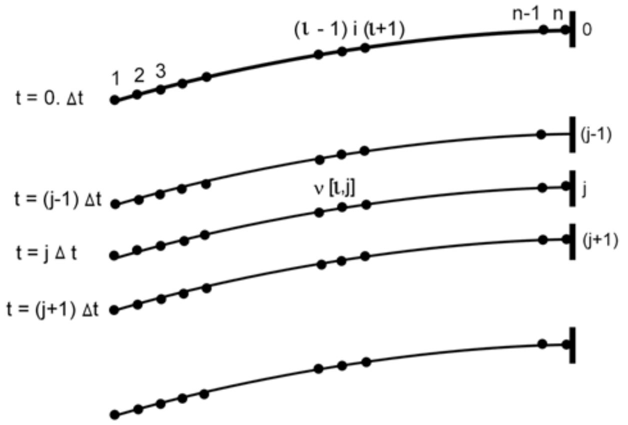

Figure 3. Beam represented by finite difference model.

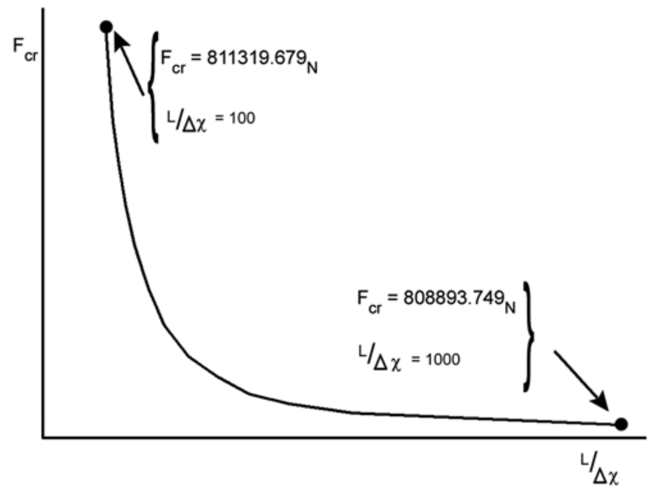

Figure 4. Convergence of critical load with mesh size.

BOUNDARY CONDITIONS IN FINITE DIFFERENCE FORMS

The boundary conditions were stated above, i.e. the clamped end and the internal supports, are used in the present analysis. Consequently, the boundary conditions stated in eqn (28), in finite difference form are given bellow:

$$\upsilon_{(x,t)} = \sum_{i=o}^{\frac{x}{\Delta x}} \upsilon'_{(i\cdot\Delta x,t)} \cdot \Delta x \quad (33)$$

$$\upsilon'_{(x,t)} = -\sum_{i=\frac{x}{\Delta x}}^{\frac{L}{\Delta x}} \upsilon''_{(i\cdot\Delta x,t)} \cdot \Delta x \quad (34)$$

CONVERGENCE STUDY

In order to establish the degree of accuracy of the results, a convergence study is carried out. The number of nods which is characterized by the ratio (L/Δx) varies from 3 to 1000 and the percentage of error is shown in Table 1. The convergence curve for the critical load is shown in Figure 4. In Figure 4 as the number of nodes increases, the critical load converges to a fixed value. As shown in Table 1, with increasing the number of nodes the percentage of error induced reaches to a practically negligible value. This is obviously expected to happen. The relative error is calculated from the following relation:

$$\text{Error} = \frac{\left|F_3 - F_{cr}\right|}{F_{cr}} \quad (35)$$

Table 1. Percentage relative error.

Number of nodes L/Δx	3	4	5	10	100	1000
Percentage relative error	4.7	2.6	1.6	0.4	0.003	0.00003

NUMERICAL RESULTS AND DISCUSSION

The numerical results obtained from the solution of the governing equations include the Euler-Bernoulli and Timoshenko beam results. Initially the results are compared with existing results in the literature and, following the comparison of the results, several new results particularly for Timoshenko beams are presented. It is worthwhile mentioning that, if desired, in order to obtain Euler-Bernoulli beam result one may eliminate the shear term in the Timoshenko beam theory.

Comparison of Results

The results for viscoelastic buckling of E-B and Timoshenko beams are presented in Table 2 for comparison purposes. The properties used in computing the results are given bellow:

$I = 160 \quad 10^{-6}$ m^4, L = 10 m, n = 1.2 (used only for Timoshenko beam), E = 200 GPa , A = 0.001 m^2, η = 0.001 (kg/m.s), $P^v = 1$, $Q^v = 0$

Here, in fact, the Poisson's ratio is set to zero which is

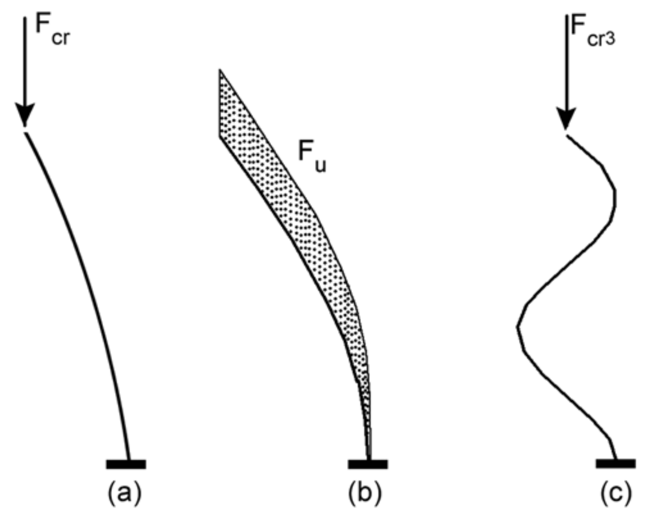

Figure 5. Examples for E-B and Timoshenko beams, (a) E-B and Timoshenko, (b) and (c) Timoshenko.

a legitimate assumption in viscoelastic beams. The type of examples solved is shown in Figure 5.

In Figure 5c, a cantilever subjected to a concentrated axial load in its third buckling mode is shown. For solving this type of problems internal boundary conditions are required. This type of internal supports is stated in eqn (29). The results are given in Table 3.

As seen from the results presented in Tables 2 and 3 the results obtained from the finite difference numerical solution correlate very well with the exact theoretical results.

New Results

In this section seven new examples of the type of Timoshenko beam are solved. The properties used are the same as those used above.

Table 3. Critical load comparison for example Figure 6c for $\Delta t = L/n = 10/500$, $\Delta t = 0.421 \times 10^{-10}$s, Error $\leq 10^{-5}$.

Example	Present	Reference [10]
Figure 5 (c) Timoshenko	20222538.28 N	20222336.05 N

Example One

The buckling of a cantilever beam with Kelvin type solid model is considered under the loading shown in Figure 6.
The loading profile is defined as:

$$F_{(x)}=F_{crd}\cdot(x/L)(N/m)$$

when (F_{crd}) is the magnitude of the uniformly distributed critical load which is obtained to be (1063033.301(N/m)) with ($\Delta t = 5\ \ 10^{-11}$s) and the error is within (10^{-5}). Employing the implemented theory and the techniques the critical load profile is found to be as follows:

$$F_{(x)}=1063033.301\times(x/L)(N/m)$$

Examples Two to Six

In examples two to six a similar critical load profile is found as follows:
For example two: $F_{(x)} = 344912.262 \times (x/L)(N/m)$
For example three: $F_{(x)} = 280228.604$ (N/m)

Table 2. Critical load comparison for examples in Figures 5a and 5b.

Examples	Present results	Reference [10]
Figure 5 (a) E-B beam $\Delta t = 7.332 \times 10^{-10}$s, $\Delta x=\frac{L}{n}=\frac{10}{200}$ Error $\leq 10^{-5}$	789568.352 N	789575.529 N
Figure 5 (a) Timoshenko $\Delta t = 7.332 \times 10^{-10}$s, $\Delta x=\frac{L}{n}=\frac{10}{200}$ Error $\leq 10^{-5}$	808901.531 N	808893.442 N
Figure 5 (a) Timoshenko (n=1000) $\Delta t = 7.332 \times 10^{-10}$s, $\Delta x=\frac{L}{n}=\frac{10}{1000}$ Error $= 3 \times 10^{-5}$	808893.842 N	808893.442 N
Figure 5 (b) Timoshenko $\Delta t = 6.259 \times 10^{-10}$s, $\Delta x=\frac{L}{n}=\frac{10}{200}$ Error $\leq 10^{-5}$	258651.0 N/m	258649.278 N/m

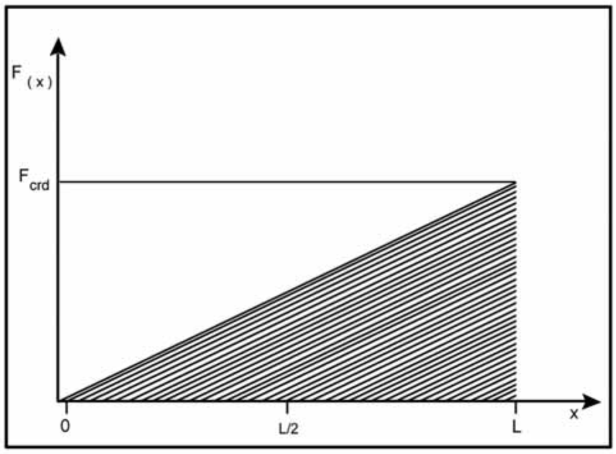

Figure 6. Distributed loading in the form of increasing ramp along the beam.

For example four: $F_{(x)}$ = 453313.259 × (L-2x)/L(N/m)
For example five: $F_{(x)}$ = 720270.436 × (2xL)/L(N/m)
For example six: $F_{(x)}$ = 346782.311 × (L-x)/L(N/m)

Consequently the critical load can be calculated at a desired position along the beam. The complete results are summarized in Table 4.

Example Seven

In this problem a cantilever beam under a general axial loading as shown in Figure 7 is considered. The general loading is defined as follows:

(F_1) is applied at $x_1 = 0$ m
(F_2) is applied at $x_2 = 0.2$ m
(F_3) is applied at $x_3 = 0.4$ m
(F_4) is applied at $x_4 = 0.7$ m

and (F_5) is a non-uniformly distributed load. The mechanical and geometrical properties are given as follows:

I = 160 × 10^{-6}, E = 200 GPa, η = 0.001 (kg/m.s), L = 1 m, A = 0.001 m^2, $P^v = 1$, $Q^v= 0$, n = 1.2, and specifying $\rho = 0$ shows that the problem is a quasi-static one.

(a) (F_{cr}) is assumed to be the critical axial load applied at the free end, then let: (F_1= 0.5 F_{cr}), (F_3= 0.2 F_{cr}), (F_4= 0.3 F_{cr}), and F_5 = (1/meter^3) × x(x-0.5)F_{cr} (0m ≤ x ≤ 0.6 m). (F_{2cr}) should be determined for the equilibrium of the beam.

(b) If at time (t = 0) the initial deflection of the beam is:

$$\upsilon_{(x,0)} = 10^{-3} \times \sin(\frac{x}{L}.\frac{\pi}{2})(\text{meter})$$

and

$$\left.\frac{\partial^i \upsilon_{(x,t)}}{\partial t^i}\right|_{t=0} = 0, (i=1,2,3,...)$$

and (F_2 = 10F_{2cr}) and the other loads are similar in magnitude and position to those defined in (a) determine the time that it takes for maximum slope of the beam to reach a value of (0.06) from its initial value.

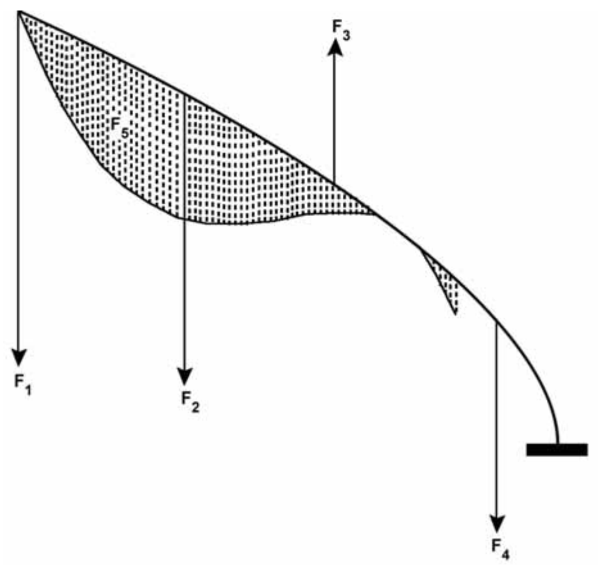

Figure 7. Beam and its loading for example seven.

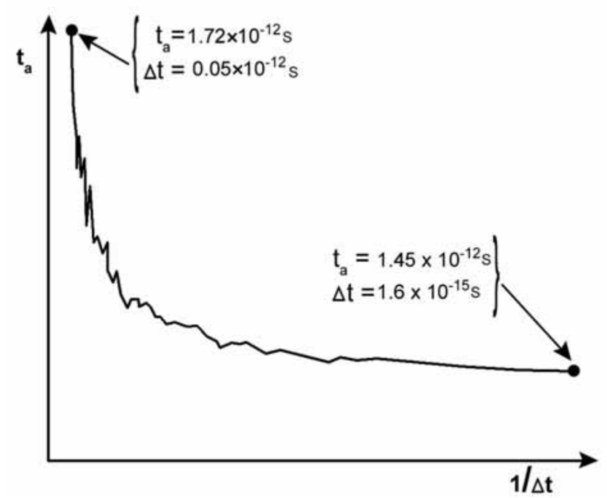

Figure 8. Convergence analyses for part (b).

Table 4. Critical load profile results for various loading conditions for cantilever Timoshenko beams.

New examples	Critical load profile	Loading condition
Example one:	$F_{(x)}$=1063033.301×(x/L)(N/m)	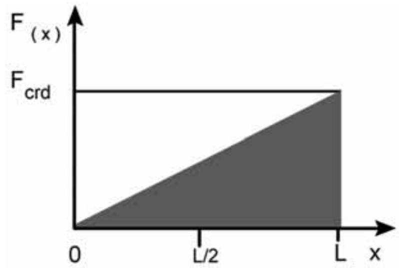
Example two:	$F_{(x)}$= 344912.262 ×(x/L) (N/m)	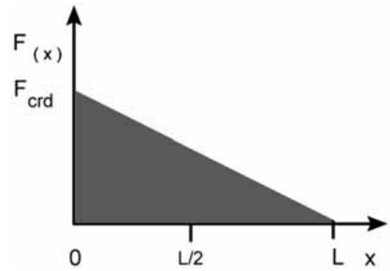
Example three:	$F_{(x)}$= 280228.604 (N/m)	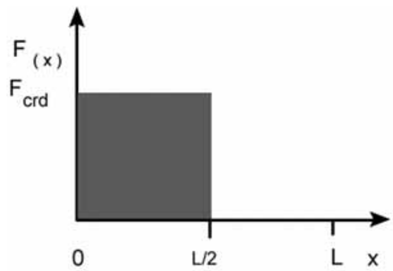
Example four:	$F_{(x)}$= 453313.259 ×(L–2x)/L(N/m)	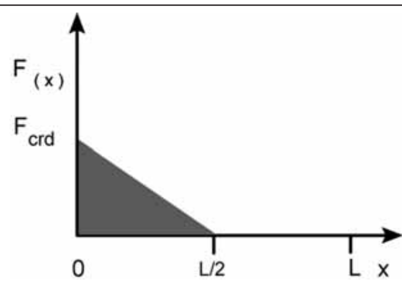
Example five:	$F_{(x)}$=720270.436×(2x/L)(N/m)	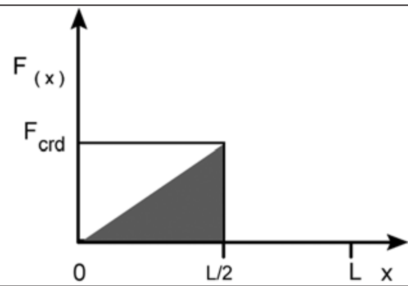
Example six:	$F_{(x)}$=346782.311×(L–x)/L(N/m)	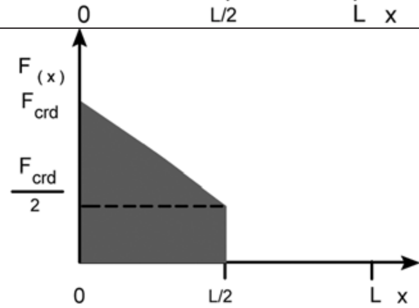

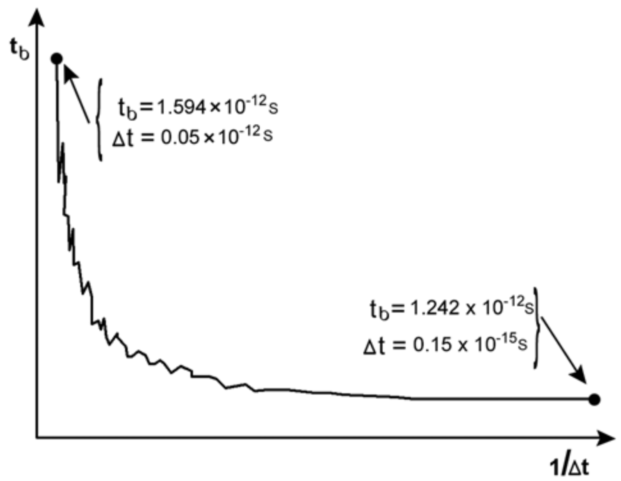

Figure 9. Convergence analyses for part (c).

(c) If the initial deflection at time (t = 0) is given as follows:

$$\upsilon_{(x,0)} = 10^{-3} \times \sin(\frac{x}{L} \cdot \frac{\pi}{2})(\text{meter})$$

and

$$\left. \frac{\partial^i \upsilon_{(x,t)}}{\partial t^i} \right|_{t=0} = 0, (i = 1, 2, 3, ...)$$

and that

$$F_2 = 10F_{2cr} + F_{2cr}/10.t.(1/s)$$

and all the other forces are the same as above, again, determine the time that it takes for the maximum slope to reach a value of (0.06) from its initial value.

Solution for (a)

Initially (F_{cr}) is found to be ($584.52\ 10^6$ N) for (Δx = 0.01 m) and ($\Delta t = 10^{-15}$ s). In part (a) (F_2) is set to ($F_2 = 0$) and check for the stability of the beam and that it is found to be stable. Therefore, a critical value for (F_2) can be obtained. Using the procedure described earlier the critical value for (F_{2cr}) is found to be ($F_{2cr} = 0.61235F_{cr}$).

Solution for (b)

Having found (F_{cr}) and (F_{2cr}), the loading profile is known. This loading and the boundary conditions for t = 0 are applied and the required time is found to be (t_a = $1.4442\ 10^{-12}$s) and that the maximum slope is at (x = 0). The accuracy of this result is specified by the convergence study as shown in Figure 8. For the above results (Δt) is taken to be ($\Delta t = 0.3\times10^{-15}$s).

Solution for (c)

Similarly (F_{cr}) and (F_{2cr}) are calculated. Applying the loading and the boundary conditions at (t = 0), the required time is computed to be (t_b) for $t_a = 1.2415\times10^{-12}$s. The convergence of ($t_b$) is shown in Figure 9.

CONCLUSION

The differential and integral forms of the Euler-Bernoulli and Timoshenko beams governing equations with time-dependent axial and transverse loadings are developed. The loading on the Euler-Bernoulli beam can be axial and simultaneously transverse of a general type. However, the loading on the Timoshenko beam can be pure axial but still of a general nature. The mechanical properties for a Kelvin type material model are defined. The boundary conditions are successfully implemented. The equations developed here determine the deflection profile under the prescribed loading. Consequently, a method for calculating the critical buckling load is used. The finite difference numerical method is utilized to solve the differential forms of the beam equations and a computer program is developed to generate the numerical results. The comparisons of the present results with the existing available results are very satisfactory. Seven examples are presented with loading profiles to be used for predicting the buckling loads. Consequently, the outcome of the present paper is two fold:

(a) the nature of the general type of loading and (b) the special mathematical technique used to calculate the critical buckling loads.

ACKNOWLEDGEMENTS

The authors would like to express their sincere thanks to the Mechanical Engineering Department, Amir Kabir University of Technology for supporting this research.

NOMENCLATURE

A : Beam cross sectional area

E : Modulus of elasticity
F_{cr} : Critical buckling load
F_{crd} : Uniformly distributed critical load
$F_{(x,t)}$: Axial loading profile
G : Shear modulus of elasticity
I : Second moment of area
$I_{(x,t)}$: Second moment of area as function of x and t
$J^E_{(t)}$: Creep compliance function for normal deformation
K,K′: Mechanical properties of the elastic supports
L : Beam length
M: Total bending moment
M^F: Bending moment due to axial load
M^q: Bending moment due to transverse load
$M_{(x,t)}$: Total bending moment as function of x and t
n : Shear correction factor
N : Internal axial force
P^E,Q^E : Differential operators
$\bar{P}^G$,$\bar{Q}^G$: Differential operators in Laplace space
$q_{(x,t)}$: Transverse loading profile
t : Time
t_f : Final time
t′ : Dummy variable of integration
$\upsilon_{(x,t)}$: Deflection as function of x and t
$\upsilon'_{(x,t)}$: First derivative of deflection w.r.t.x as function of x and t
$\nu''_{(x,t)}$: Second derivative of deflection w.r.t.x as function of x and t
$\upsilon^M_{(x,t)}$: Deflection due to bending
$\upsilon^S_{(x,t)}$: Deflection due to shear
x : Position along the beam
x′ : Dummy variable of integration
ε_{xx} : Normal strain
τ_{xx} : Normal stress
η : Viscosity coefficient
Δ( ) : Incremental value of the variable ( )

REFERENCES

1. Timoshenko S.P., Gere J.M., *Theory of Elastic Stability: The Maple*, 1961.
2. Qiao P., Barbero E.J., Davalos J.F., *On the Linear Viscoelsticity of Thin-Walled Laminated Composite Beams*, Dept. of Civil and Environ. Eng., West Virginia University, Morgantown, WV., 2002.
3. Johnson A.R., Tessler A., *A Viscoelastic Higher-order Beam Finite Element*, Technical report, Computational Structures Branch, NASA Langley Research Centre, MS 240, Hampton, VA 23681-0001, 1996.
4. Yu S.D., *Creep Bending of Linear Viscoelastic beams Subjected to Axial and Transverse Loads*, the 18th CANCAM, St. John's Newfoundland, June 3-7, 2001.
5. Chen T.M., The hybrid Laplace transform/finite element method applied to the quasi-static and dynamic analysis of viscoelastic Timoshenko beams, *Int. J. Num. Methods Eng.*, **38**, 509-522, 1995.
6. Lin Z.M., Polyzois D., Shah A., Nonlinear analysis of fibre-reinforced plastic poles, *Stru. Eng. Mech.*, **6**, 785-800, 1998.
7. Ibrahim S., Polyzois D., Ovalization analysis of fibre-reinforced plastic poles, *Comp. Stru.*, **45**, 7-12, 1999.
8. Shames I.H., Cozzarelli F.A., Elastic and inelastic stress analysis, *Prentice Hall*, 1992.
9. Hlavacek I., *Buckling of a Timoshenko beam on elastic foundation with uncertain input data, IMA, J. Appl. Math.*, **68**, 185-204, 2003.
10. Flugge W., Viscoelasticity, *Springer-Verlag*, Berlin, 1975.